CRITICAL REVIEW OF THE DESIGN OF SPACE ENVIRONMENT SIMULATORS: LESSONS LEARNT

J. I. Kleiman, S. Horodetsky, V. Sergeyev, V. Issoupov, R. Ng

ITL Inc., 80 Esna Park Drive, Units #7-9, Markham, ON, L3R 2R7 Canada
Phone: 1-905-415-2207, Fax: 1-905-415-3633, Email: <jkleiman@itlinc.com>

ABSTRACT

In an attempt to develop a simulator facility that would be adaptable to routine, reliable, not expensive long-term testing of materials, systems and components, ITL Inc. has designed and manufactured several prototypes of a Multifunctional Environment Simulator (MES™) facility that use the common principles of formation of continuous and pulsed AO beams. In designing of the MES™ that, generally, contains the following three major modules: vacuum chamber and pumping system; physical sources of LEO factors for accelerated testing and characterization; and an advanced computerized operational and control module, a number of requirements had to be satisfied, some of them simultaneously. One of the critical requirements to the MES™ vacuum chamber is to maintain maximum possible axial symmetry of all mounted LEO space-factor sources to provide simultaneous maximum interaction of the factors. Another requirement was to minimize the internal volume of the vacuum chamber to allow for optimization of the design and working parameters of the vacuum and pumping systems.

1. INTRODUCTION

Atomic oxygen sources are used commonly for ground-based accelerated testing and qualification of external spacecraft materials and coatings [1-19]. However, due to general complexity of the ground-based simulation testing, the atomic oxygen simulation techniques used around the world are known to have various drawbacks and limitations (low energy of produced O atoms, high levels of vacuum-UV radiation accompanying the pulsed AO beams, incapability of simulation of the synergistic effect of various space factors, difficulty to perform *in-situ* measurements, etc.) [4, 7, 8]. The existing AO simulators many times rely on costly and short lifetime components that considerably affect the reliable long-term operation of such systems and increase the costs associated with such testing programs. Thus, for reliable continuous operation of the fast gas valves in laser pulsed AO systems used by many groups around the world, lasers with 7-12 J energy are required [7, 16, 20-27]. The practice had shown that such sources stop to operate reliably when the laser energy drops to ~6 J. The existing mechanical pulsed valves as well as use of sophisticated piezoelectric pulsed valves also proved to be cumbersome and expensive. Therefore, it is critically important to find new technological approaches to testing methodologies and equipment for ground-based simulation experiments.

Simulation of the LEO space environment produces a number of strict technological and physical criteria to individual factor sources. The testing must be performed in vacuum better than 10^{-5} torr provided by oil-free pumping. The vacuum chamber geometry should allow for simultaneous exposure to various space factors and *in-situ* monitoring of physical properties of the irradiated materials, as well as physical parameters of individual simulated factors (Time-of-Flight, QCM, atomic emission spectroscopy, etc.). Material's interaction with atomic oxygen in its main ground state $O(^3P)$ with thermal and hyperthermal energies is essential for studying materials behavior in LEO environment. As shown by many authors [18-21], AO effects on materials depend on eventual AO/UV synergistic irradiation, therefore, the wavelength range of UV delivered by the UV source has to be from 115 to 400 nm; i.e. include the radiation range producing the most important effects on polymer materials. The above conditions are often combined with thermal treatment (hold at a given temperature, temerature ramp or thermal cycling) representative of temperature conditions met by materials in LEO. Other optional space factor sources (protons, electrons, ions, contamination sources) can be mounted on available flanges to expand the MES™ applications to GEO and MEO orbits.

This paper is a critical review of the experience gained at ITL Inc. during the design of a new multifunctional environmental simulator facility. Technical criteria for development of the simulator facility were formulated based on optimization of existing conventional and original new designs. Along with required technical specifications, the cost factor was considered as one of the most important optimization parameters. A novel MES™ design should allow accommodation of larger samples like parts of large space structure (satellites, etc.) of any complicated geometry. Moreover, as far as material's exposure to the above factors is provided by simultaneous operation of various sources, the MES™ facility has to be controlled by powerful user-friendly operational software and be able to function in

automatic mode without much attention from the MES™ operator.

2. DESIGN OF EXPERIMENTAL FACILITY

The MES™ is designed to conduct ground-based testing and characterization of spacecraft materials and coatings under simulated conditions of high vacuum, fast atomic oxygen, VUV and NUV radiation, and temperature cycling. The basic simulator system contains the following specific components: a) Vacuum System; b) Sample Positioning and Manipulation System; c) Pulsed laser-assisted AO Source and continuous RF-assisted AO Source; d) VUV/NUV Radiation Sources and e) Central PLC computer Control System. As an option, the MES™ facility allows for installation of sources of accelerated monoenergetic electrons and protons. The MES™ chamber is equipped with measurement and analytical instruments that include a QCM monitor and a ToF system, video-camera, and has a number of ports for attaching additional *in-situ* characterization systems.

One of the important components of the MES™ system is the originally designed high vacuum chamber. The MES™ vacuum chamber is cylindrical in shape with one of its ends having a semi-spherical basis. This design permits installation of individual space factor sources on the semi-spherical basis. Samples, when mounted on the sample-holder are positioned in the focal plane of the semi-sphere and are exposed to simultaneous solar UV and NUV irradiation and normal incidence exposure by AO neutral beams.

The main components of the AO laser source are the pulsed CO_2 IR laser, optical system, gas introduction system and synchronization system. The LASERPULSE 2500 CO_2 IR laser produces electromagnetic pulses at 10.6 μm with a pulse energy of ~5.5 J and pulse length of 250 ns. Interaction of fast AO with spacecraft materials is simulated in a high vacuum chamber ((1) in Fig. 1) made of stainless steel. The vacuum chamber is pumped using a Varian TV 1001 Navigator turbo pump (1000 l/min pumping speed) and an auxiliary rotational DS-602 mechanical pump (18.3 cfm pumping speed).

The gas introduction system includes a high-pressure O_2 cylinder, high-pressure reductor, tubing system, high-pressure gas chamber (2) with security gauge and pulsed valve (3) (Fig. 1). Molecular oxygen is introduced into the conical nozzle (10) with a 20° full included angle at a pressure of 100-500 psi. As the gas begins to expand into the nozzle, the laser is fired 150-400 ns after gas pulse and it initiates a plasma heated to more than 20,000 K. Electron-ion recombination in the expansion is very efficient; thus, the resulting beam consists of neutral atomic and molecular oxygen with an ionic component less than 1%. The pressure in the vacuum chamber is increased from 10^{-7} to $4 \cdot 10^{-5}$ Torr for the duration of the gas pulse and returns to 10^{-6} Torr as soon as the introduced gas is pumped out, before introduciton of the next gas pulse. Influence of the time delay between the gas pulse and the laser pulse on the velocity and mean energy of neutral and charged particles in the generated beam is characterized and discussed in [26-28].

In case of lateral delivery of the laser beam in the AO source (Fig. 1a), the laser pulse is delivered into the MES™ chamber via the optical system consisting of a lightguide, ZnSe portview (6), and a set of IR mirrors, focused by a ZnSe lens with 500 mm focal distance (5) that is adjusted using a focusing system (4). A flat molibdenum mirror (7) fixed on a step-motor computer controled mirror support (8) allows the incidence angle of the laser beam to be adjusted between 10° and 12° and the laser pulse to be reflected into the conical nozzle (10). Samples exposed to atomic oxygen beam are located on the sample-holder (9).

In the coaxial AO source (Fig. 1b) the laser beam delivery system is designed differently. In this case, the source operates without the optical system and IR mirrors, and the ZnSe focusing lens is used as a portview at the same time. Due to such modification, the laser beam energy losses could be minimized from 12.7% to 2.3% (Table 1). Samples exposed to atomic oxygen beam are located on the sample-holder (9).

The pulse energy of the CO_2 IR laser was measured using a GENTEC Joulemeter JAI-2 providing the relation between the applied energy and the voltage response across the load resistor. The pulse energy varies as a function of high voltage (32 to 35.5 kV) applied to the discharger of the LASERPULSE 2500 laser.

3. EXPERIMENTAL

To determine the effective atomic oxygen fluence, witness samples of vacuum dehydrated Kapton 200 HN with a surface area of 1 × 1" were exposed to the atomic beam in the same facility. The AO effective flux and the AO fluence were calculated according to the ASTM standard [29] based on the mass loss of the witness material due to erosion by AO. The mass loss of the witness samples as a function of time of exposure to AO was controlled using an electronic balance with an accuracy of 10^{-5} g.

A number of characterization methods have been used to evaluate the changes in surface morphology. Scanning Electron Microscopy/Energy Dispersive Spectroscopy (SEM/EDS) have been used for material erosion, performance, and durability evaluation. The SEM/EDS was mostly used to study the surface morphology and elemental composition of the

investigated samples. SEM studies were performed on a JEOL JSM-T300 model microscope.

4. DISCUSSION

4.1 Vacuum Chamber

Based on the criteria for simulation of the LEO space environment, the vacuum chamber is manufactured from stainless steel with all vacuum connections (flanges) designed for high-vacuum conditions. The spherical design of the vacuum chamber allows the highest degree of symmetry for all flanges, thus facilitating the alignment of various factors for simultaneous exposure. To allow for easy sample exchange and for exposure of an object of any complicated geometry, the vacuum chamber may combine two independent ways of samples exchange: an access door/port for routine sample exchange and a two-part, detachable chamber design for installation of larger samples.

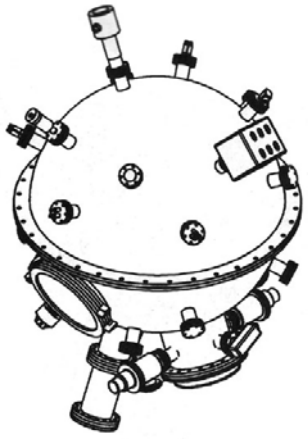

Figure 1. Spherical design of the vacuum chamber

The spherical shape of the chamber with its symmetrical geometry would provide the most effective design for installation of individual sources of the related LEO environmental factors and laboratory instrumentation. The chamber would also be extendable, i.e. will permit installation of additional irradiation sources, such as electron and proton sources, contamination sources, laser or electron heating systems, measurement and control equipment for *in-situ* monitoring of optical, mechanical, electrical, thermophysical and morphology parameters of the materials during exposure.

When using the detachable chamber design (Fig. 1), the chamber consists of front and back hemispheres. This design would allow minimizing the internal volume of the vacuum chamber to allow for optimization of the design and working parameters of the vacuum and pumping systems. All flanges are of ConFlat (CF) type with copper gaskets seals. The disadvantage is the limitations imposed to the size and geometry of the sample that could be put inside.

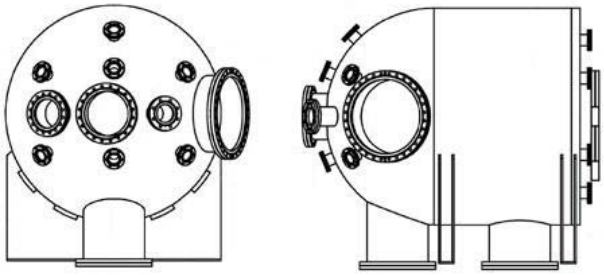

Figure 2. Semispherical cylindrical MES™ vacuum chamber

Another chamber design involved a combination of a semisphere with a cylindrical chamber (Fig.2). The advantage of the semispherical-cylindrical vacuum chamber in Fig. 2 is the maximum possible axial symmetry of all mounted LEO space-factor sources to provide simultaneous maximum interaction of the factors with an increased volume that allows for testing of larger samples. The base of the cylinder is a flap door to allow for easy access and accommodation of materials and structures to be tested in the MES™. This chamber has a volume of about 0.8 m^3 (1.5 times the volume of the spherical design) and, therefore, it is more attractive for laboratory testing.

4.2 Pumping System

The vacuum chamber is pumped with a turbo pump (Varian TV 1001 Navigator) and two auxiliary rotational mechanical pumps (DS-402 and DS-602). The DS-402's and DS-602's pumping speed is 12.3 cfm and 18.3 cfm, respectively. The pumping speed of the Varian TV 1001 Navigator turbo pump is 1000 l/min.

4.3 Laser AO Source

The main components of the AO laser source (Figs. 3, 4) are the CO_2 IR laser with the optical system, pulsed gas valve, conical nozzle and the synchronization system. The LP 2500 CO_2 IR laser produces electromagnetic pulse at 10.6 μm with a pulse energy of ~5.5 J and pulse length of 250 ns. Molecular oxyegn is introduced into a high-pressure gas chamber (2) with a security gauge and then is injected through the pulsed valve (3) into the conical nozzle (10) with a 20° full included angle at a pressure of 100-500 psi. As the gas begins to expand into the nozzle, the laser is fired 150-400 ns after gas pulse and initiates a plasma, heated to more than 20,000 K. The laser-induced breakdown of molecular oxygen is used in many AO similation facilities around the world [16, 26,

27, 30-32]. Electron-ion recombination in the expansion is very efficient; thus, the resulting beam consists of neutral atomic and molecular oxygen with an ionic component less than 1%.

The pressure in the vacuum chamber is increased from 10^{-7} to $4 \cdot 10^{-5}$ Torr during gas pulse and returns to 10^{-6} Torr as soon as the introduced gas is pumped out before the next gas pulse. Influence of the time delay between the gas pulse and the laser pulse on the velocity and mean energy of neutral and charged particles in the generated beam are characterized and discussed in [28]. The main technical parameters of the two prototypes of the deeloped AO source are summarized in Table 1.

In case of lateral delivery of the laser beam in the AO source (Fig. 3a), the laser pulse is delivered into the MES™ chamber by means of the optical system consisting of a lightguide, ZnSe portview (6), and a set of IR mirrors, focused by a ZnSe lens with 500 mm focal distance (5) adjusted using a focusing system (4). A flat molibdenum mirror (7) fixed on a step-motor computer controled mirror support (8) allows the incidence angle of the laser beam to be adjusted between 10° and 12° and the laser pulse to be reflected into the conical nozzle (10). Samples exposed to atomic oxygen beam are located on the sample-holder (9).

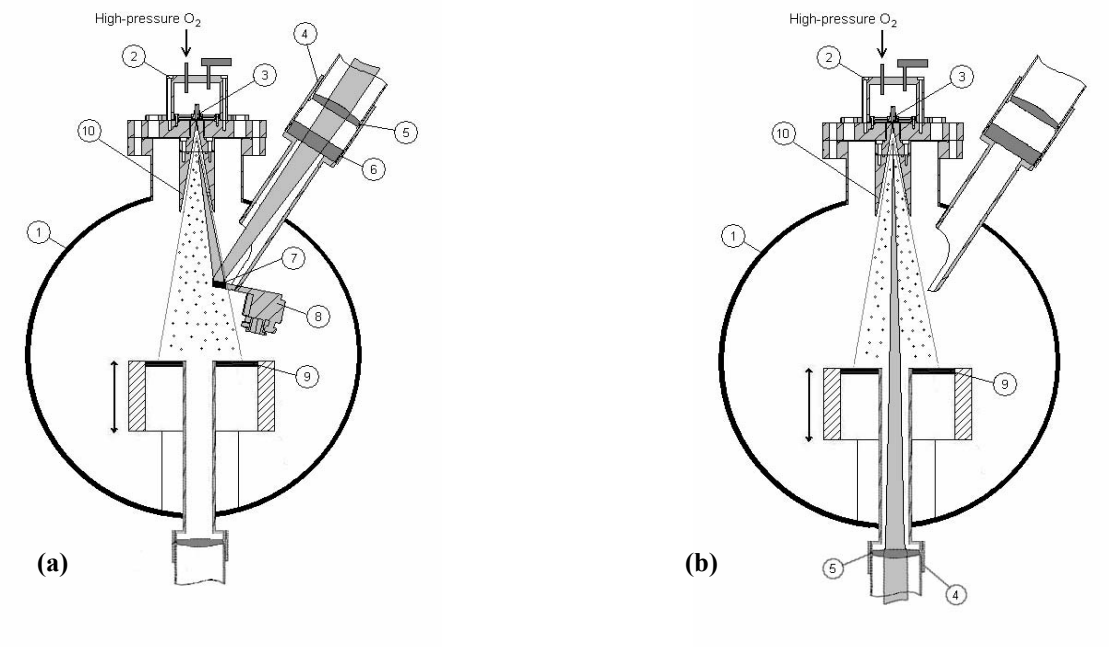

Figure 3. Schematic presentation of the lateral (a) and coaxial (b) laser AO sources.

Table 1. Technical specifications of the lateral and coaxial AO sources of the MES™ facility

#	Technical parameter	Working value	
		Lateral laser AO source	**Coaxial laser AO source**
1	Distance between the laser and the focusing lens (cm)	120	270
2	Laser pulse energy loss (%)	12.7	2.3
3	Nominal energy density (J/cm^2)	5 to 6 (before focusing) 250 to 310 (after focusing)	5 to 6 (before focusing) 320 to 410 (after focusing)
4	Laser beam section (mm^2)	25.4×25.4 (before focusing) 3.5×3.5 (after focusing)	25.4×25.4 (before focusing) 5×5 (after focusing)
5	Power density (MW/cm^2)	7.8 (before focusing) 410 (after focusing)	7.8 (before focusing) 200 (after focusing)
6	AO energy range (eV)	0-14.5	4.7.-14.5
7	AO max. flux at 4 Hz ($atoms/cm^2/s$)	$2.4 \cdot 10^{15}$	$1.5 \cdot 10^{16}$
8	Distance to samples (cm)	22-60	22-60
9	Max. sample size and geometry	Disk 225 mm^2 or parallelepiped 200×200×400 mm^3	Disk 225 mm^2 with a central hole of 50 mm in diameter

In the coaxial mode of the AO source (Fig. 3b), the difference consists in the configuration of the laser beam delivery system. In this case, the source operates without the optical system and IR mirrors, and the ZnSe focusing lens is used as a portview at the same time. Due to such a modification of the source, the laser beam energy loss could be minimized from 12.7% to 2.3% (Table 1). Samples exposed to atomic oxygen beam are located on the sample-holder (9).

The MES™ facility is fully computer-controlled and operated by original Atomic™ software. It is used for all operations that a researcher might want to undertake: control the main parameters of the MES™ sources, start new experiments, view saved reports and manage other user's access privileges. The general schematics of the MES™ facility including the lateral AO source are shown in Fig. 4.

4.4 Microwave AO Source

In contrast to the laser AO source, the microwave AO source generates continuous flux of atomic oxygen. When developping the microwave AO system of the MES™, we reviewed all know conventional designs (Surfatron [33], Resonance RF Plasma Source [4], and Plasma Source [34, 35]) and employed the commercial highly reliable AX7610 microwave plasma source creating a unidirectional neutral beam of atomic oxygen. The MES™ microwave plasma system is mounted on a 6" ConFlat flange (7) as shown in Fig. 4.

A differential pumping system provides high vacuum conditions in the MES™ chamber during plasma source operation under a working pressure of 1-8 Torr. With a quartz plasma tube, the AX7610 downstream source is ideally suited for production of atomic oxygen with energies up to 0.5 eV. The patented conductively-cooled design of the plasma tube (388 mm length, ∅25 mm) supports high throughput and high power (up to 2 kW) operation. The wide process window allows for AX7610 use in multiple applications and it is used as part of MES™ microwave plasma system that also includes a microwave power generator, waveguide components, and a three-stub manual tuner. The microwave power is delivered through the isolator, which re-directs and absorbs reflected microwave energy protecting the magnetron. The system includes a bidirectional coupler to measure the actual microwave power and to provide tuning feedback. The microwave source generates and sustains atomic oxygen plasma inside the plasma source.

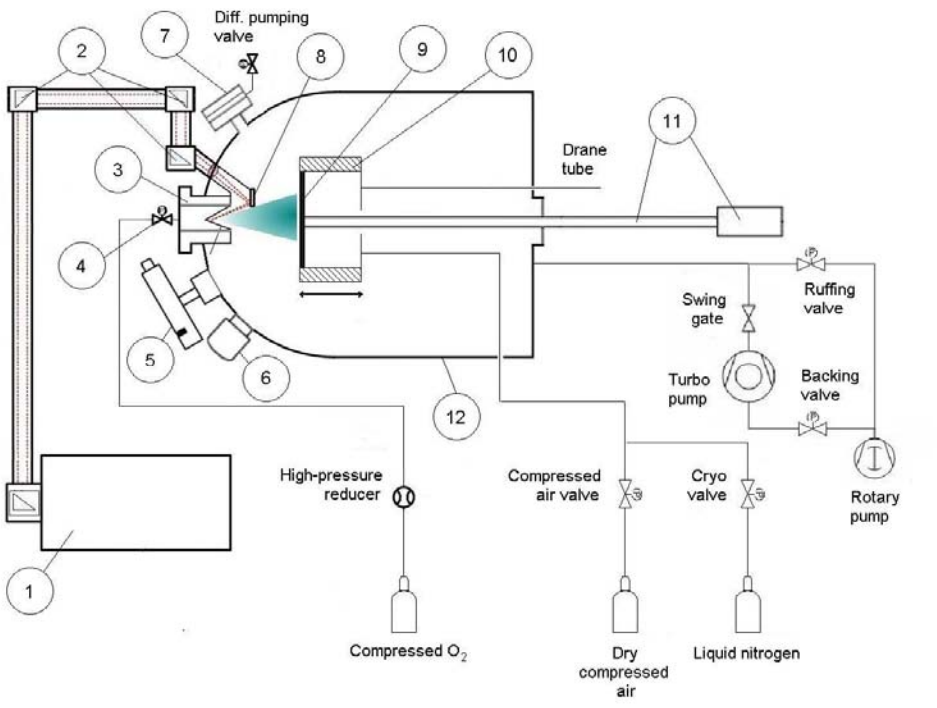

Figure 4. Schematic of the MES™ facility: 1 - CO_2 IR laser; 2 - IR mirrors; 3 - O_2 injection tube; 4 - pulsed valve; 5 - NUV source; 6 - VUV source; 7 - microwave AO source; 8 - molybdenum adjustable mirror; 9 - sample holder plate; 10 - heating/cooling nest; 11 - Time-of-Flight system, 12 - high vacuum chamber

4.5 VUV/NUV Sources

The VUV source (6) in Fig. 4 includes: a Hamamatsu series deuterium lamp with MgF_2 window providing a continuum spectral output between approximately 115 and 200 nm; deuterium lamp housing; and power supply. The lamp housing is designed to allow easy deuterium lamp cooling and to provide full lamp protection, performance and replacement. Deuterium lamps emit only from one side and in one direction, collection is therefore easy and efficient.

The NUV source (5) in Fig. 4 can be used in studies of photo-chemical reactions, curing of polymers, degradation of the thermo-optical properties of spacecraft materials and coatings in simulated UV radiation (200 nm up to 400 nm). The NUV source uses a Mercury Xenon lamp with the characteristic UV radiation power of 20 mW/cm^2 at a distance of 500 mm in a circle of 50 mm in diameter. The lamp housing was designed to allow handy lamp installation, as well as safe operation, high performance and easy maintenance.

A number of extra flanges were designed and placed in a pattern that allows mounting of different analytical instruments like QCM thickness monitors, optical microscopes, UV/Visible/IR spectrophotometers, etc. for *in-situ* measurements and monitoring of various physical properties of the tested materials. In future, for some types of *in-situ* characterization, samples will be transferred using a robot-manipulator from the irradiation zone into the adjacent analytical chamber.

5. AO BEAM CHARACTERIZATION

Time-of-Flight (ToF) technique has been extensively used for characterization of the AO beam delivered by the lateral and coaxial AO sources as described in [36-39]. The velocity and energy of atomic species present in the beam are then simply derived from recorded ToF distributions and specific parameters of the AO system.

The flux and the accelerating factor could be estimated from comparison of the atomic oxygen flux in LEO and in the ground-based simulated conditions. At orbital altitudes of ~300-400 km, materials are subject to an effective AO flux of approximately (1-5)·10^{14} atoms/cm^2/s on ram surfaces of a spacecraft with an average collision energy of ~5 eV. To evaluate the AO fluxes produced by the AO laser sources, Kapton HN witness samples have been exposed in the MES™ chamber.

5.1 Lateral AO Source

The 3D profile of the AO flux measured using Kapton HN witness material at 40 cm from the source is presented in Fig. 5. This profile represents a 3D surface obtained by interpolation of AO flux data in different points on the sample holder.

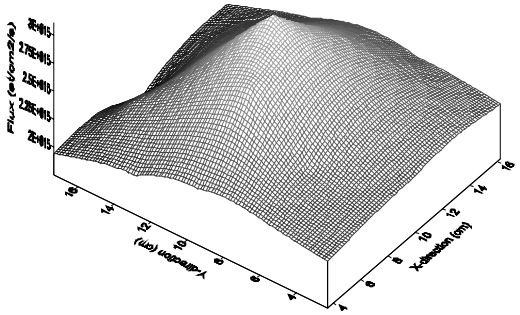

Figure 5. 3D distribution of the AO flux intensity in the sample holder plane generated by the lateral AO source at 40 cm from the nozzle. The X and the Y coordinates represent the location on the sample holder, The Z coordinate the intensity of the flux.

5.2 Coaxial AO Source

The 3D profile of the AO flux on the sample holder at 40 cm from the source is presented in Fig. 6.

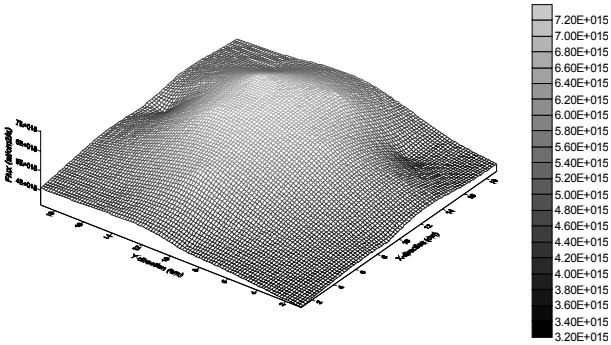

Figure 6. 3D distribution of the AO flux generated by the coaxial AO source at 40 cm from the nozzle.

6. MATERIALS EROSION TESTING

6.1 Laser AO Source

The mass loss of Kapton HN witness samples placed at 35 cm from the lateral AO source indicated that a maximum AO flux of 2.15·10^{16} atoms/cm^2/s could be obtained at a laser repetition frequency of 4 Hz. In experiments with low fluencies (1·10^{19} atoms/cm^2), loss of surface brilliance was observed during the first stages of exposure. Fluencies of 5·10^{19} to 1·10^{20} atoms/cm^2 left visible traces of surface etching. At high fluencies, during longer exposure times (for a total of up to 24 hours), the pristine Kapton HN samples were highly eroded and started to disintegrate (Fig. 7). The surface morphology/roughness and composition change observed by SEM/EDS, the time dependence of the

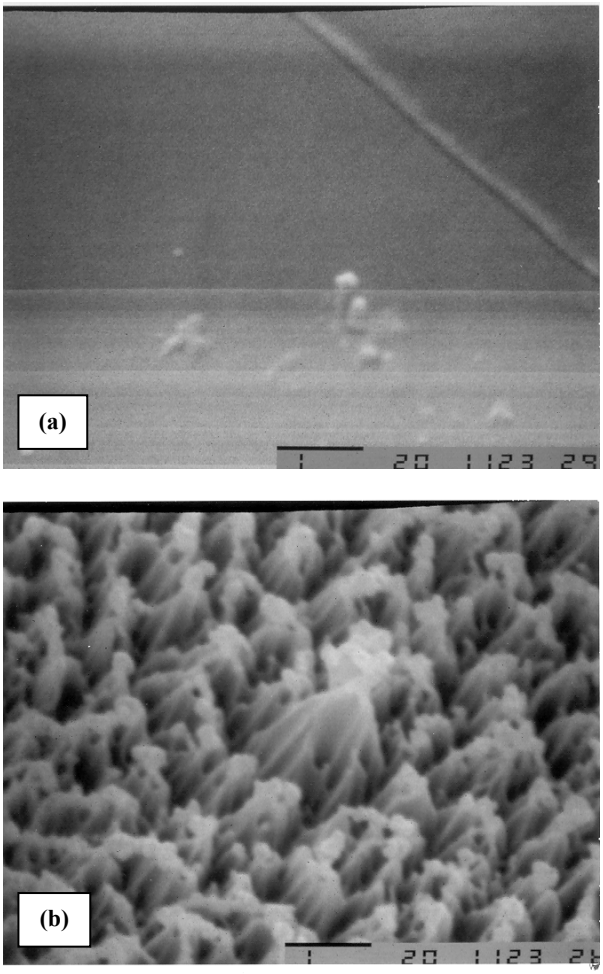

Figure7. Scanning electron microscopy analysis of a Kapton HN sample exposed to the AO flux: (a) SEM image of the masked from AO flux surface. Magnification 15,000x; (b) SEM image of the exposed to the AO flux surface. Magnification 15,000x

mass loss have been studied and confirmed the high performance of the laser AO beam source. Accelerating factors provided by the MES™ facility, as obtained in these studies, were varying between10-40.

6.2 RF AO Source

The main technical specifications of the RF continuous AO source are shown in Table 2. The average AO beam flux obtained using the AO source has been estimated to ~$(0.5\text{-}1)\cdot 10^{16}$ atoms/cm^2/s with the AO path also normal to the sample surface. Change in color and surface morphology has been obvious at visual inspection for all the samples exposed to RF oxygen plasma source. The samples exposed to microwave AO plasma looked darker, with more developed surface morphology, as shown in Figure 8.

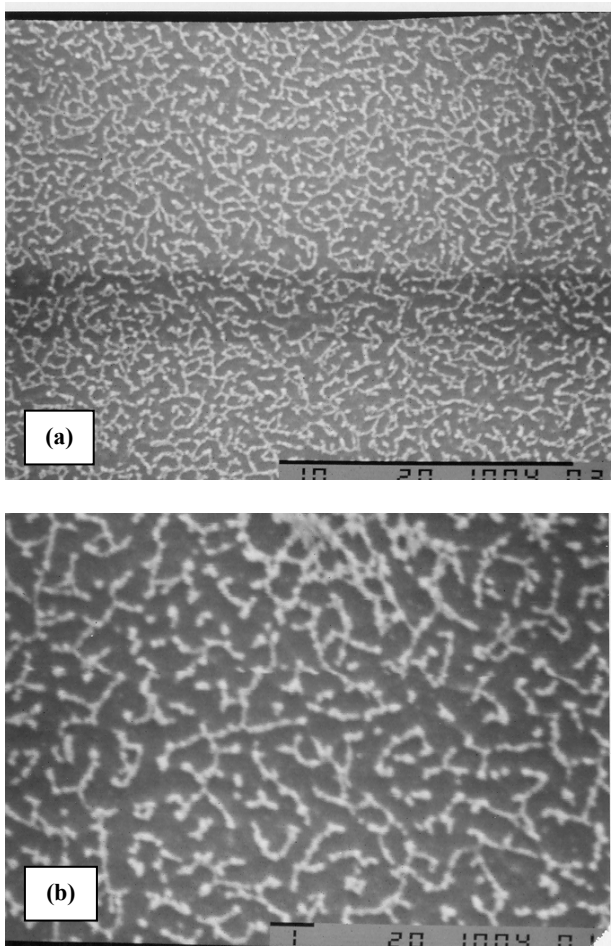

Figure 8. Scanning electron microscopy analysis of a Kapton HN sample exposed to ~6 hours of continuous AO flux using the RF continuous AO source: (a) Magnification 5,000x; (b) Magnification 10,000x

Table 2. Microwave cntinuous AO source: Technical secifications

Parameters		**Specifications**
RF Generator	Type of RF generator	Magnetron
	RF generator power (kW)	0.1-1.0
	RF generator frequency (MHz)	2450
	Type of cooling	Water
Atomic Beam	Energy (eV)	0.5-1.5
	Beam flux (atom/cm2·s)	$(0.2\text{-}1.0)\cdot 10^{16}$ at 45 cm
	AO content	~98%
	Concentration of O_2	$\leq$1%
	Concentration of O_3	$\leq$1%
	Accelerating factor	10-100

Note that the present RF AO source exposure was very close, according to its environmental conditions, to an oxygen plasma asher exposure [40]. RF oxygen plasma testing allows, in a comparatively easy way, to perform high AO effective fluence exposures, but with thermal energy AO and other oxygen plasma species, as well as uncontrolled VUV radiation.

7. CONCLUSIONS

ITL Inc. has designed and built several prototypes of Multifunctional Environment Simulator facility that could be used reliably for routine, long-term testing of materials, systems and components in simulated LEO space environments. One of the main components of the MES™ facility, the AO source, is based on common principles of formation of continuous and pulsed AO beams. The laser source is using a novel optimized fast gas valve and an inexpensive low-energy CO_2 IR laser. A number of new technological solutions were implemented and can be used in design of ground-based simulation facilities.

The lateral laser-assisted AO source provides fluxes of neutral oxygen atoms that were found to be lower than in the AO source with coaxial laser beam delivery. It should be also noted here that no attempts were made in this study to optimize either of the sources. The main advantage of the MES™ equipped with a lateral source is that it could accommodate a big sample, an electronic device or a satellite structure of any complicated design with the acceptable geometry and dimensions.

A study of the erosion kinetics of several traditional polymer materials (polyimide Kapton, Polyethylene, Teflon, HOPG, etc.) has been performed to quantify the AO beam fluxes and erosion conditions achieved in the MES™ facility. The observed surface morphology/roughness and composition change, time dependence of the erosion mass loss, as well as the materials erosion and surface recession have been considered as compelling evidence of high performance of the AO beam source with a high accelerating factor provided by the created laser AO source. The coaxial AO laser source has been confirmed to provide a neutral atomic oxygen flux up to $1.5 \cdot 10^{16}$ atoms/cm^2/s at an effective energy of ~ 5 eV. The lateral AO laser source has been confirmed to provide a neutral atomic oxygen flux up to$2.4 \cdot 10^{15}$ atoms/cm^2/s at an effective energy of ~ 5 eV.

The existing semispherical-cylindrical MES™ design could be adapted for scientific investigation by replacing the chamber with a spherical chamber formed from two hemispheres. Such design, in addition to the minimum internal volume, would allow for extended analytical capabilities due to the most effective symmetry for installation of individual sources of various LEO space factors and characterization equipment. The future development of the space environment simulation technique would employ an innovative AO source with axial delivery of laser beam combining the key features of the previous designs and providing simultaneous maximum interaction of the simulated LEO factors.

8. REFERENCES

1. Inorganic Chemistry, “Principles of Structure and Reactivity”, 4th Edition, eds: Huheey J. E., Keiter E.A. and Keiter R.L., Harper Collins College Publishers, 1993.
2. Scurat V.E., Nikiforov A.P., and Ternovoy A.I., “Investigations of Reactions of Thermal and Fast Atomic Oxygen (up to 5 eV) with Polymer Films”, *Proc. 6th Inter. Symp. On Materials in a Space Environment*, ESTEC, Noordwijk, The Netherlands, 1994, pp 183-187.
3. Koontz S.L., Albyn K., Leger L.J., “Atomic Oxygen Testing with Thermal Atom Systems: A Critical Evaluation”, Journal of Spacecraft and Rockets, v.28, #3, 1991, pp. 315-332.
4. Kudryavtsev N.N., Mazyar O.A. and Sukhov A.M., “Apparatus and techniques for the investigation of methods of generating molecular beams”, Physics-Uspekhi 36(6), June 1993, pp. 513-528.
5. Dever J., McCracken C., Bruckner E. “RF Plasma Asher Vacuum Ultraviolet Radiation Characterization and Effects on Polymer Films”. in: Proceedings of the 6th International Space conference ICPMSE-6, eds. J. Kleiman and Z. Iskanderova, Toronto, Canada, 2003, pp. 335-350.
6. Atomic and Molecular Beam Methods, Ed. Scoles G., Oxford University Press, 1988.
7. Caledonia G.E., “Laboratory Simulations of Energetic Atom Interactions Occurring in Low Earth Orbit”, in: “Rarefied Gas Dynamics: Space-Related Studies”, ed. Munts E.O., Weaver D.P., Campbell D.H., Vol.116, Progress in Astronautics and Aeronautics, AIAA, 1989, pp. 129-142.
8. Minton T. and Garton D., “Dynamics of Atomic-Oxygen-Induced Polymer Degradation in LEO”, in: Chemical Dynamics in Extreme Environments: Advanced Series in Physical Chemistry, ed. Dressler R.A., World Scientific, Singapore, 2001, pp. 420-489.
9. New Scientific Technologies in Industry”, Encyclopedia, Chief editor Kasayev K.S.; Vol.17, “Space Environment Effects on Spacecraft Materials and Equipment”, Editors Novikov L.S., Panasyuk M.I., Moscow, 2000, “Entsitech”, (in Russian).
10. Gentry W.R., “Low-Energy Pulsed Beam Sources” in: Atomic and Molecular Beam Methods, v.1. Ed.

G. Scoles, Oxford University Press, 1988, pp. 54-82.
11. Orient O.J., Chutjian A., and Murad E. "Collision of $O^-(^2P)$ Ions and O (^3P) Atoms with Surfaces", in "Materials Degradation in Low Earth Orbit (LEO)", Ed. Srinivasan V. and Banks B.A., A Publication of TMS (Minerals, Metals, Materials), 1990, pp. 87-95.
12. Brinza D.E., Coulter D.R., Chung S.Y., Smith K.O., Moacanin J., and Liang R.H., "A Facility of Studies of Atomic Oxygen Interactions With Materials Proc. 3rd Int. SAMPLE Electronics Conf., June 20-22, 1989, pp. 646-652.
13. Cross, John B. and Cremers, David A. "High Kinetic Energy (1-10 eV) Laser Sustained Neutral Atom Beam Source", *NIM*B13, 1986, pp.658-662.
14. Outlaw R.A., "Producing Essentially Pure Beam of Atomic Oxygen – by providing material which dissociates molecular oxygen and dissolves atomic oxygen into its bulk", US Patent Number 4,828,817, 1989.
15. Ferguson D.C., "Atomic Oxygen Effects on Refractory Materials", ", in "Materials Degradation in Low Earth Orbit (LEO)", Ed. Srinivasan V. and Banks B.A., A Publication of TMS (Minerals, Metals, Materials), 1990, pp. 97-105.
16. Caledonia G.E. and Krech R.H., "Studies of the Interaction of 8 km/s Oxygen Atoms with Selected Materials", ibid, pp. 145-154.
17. Cuthbertson J.W., Langer W.D., and Motley R.W., "Atomic Oxygen Beam Source for Erosion Simulation", ibid, pp. 77-86.
18. Tennyson R.C. and Morison W.D., "Atomic Oxygen Effects on Spacecraft Materials", ibid, pp. 59-76.
19. Nikiforov A.P., and Scurat V.E., "Kinetics of polyimide etching by supersonic beams consisting of atomic and molecular oxygen mixtures", *Chemical Physics Letters*, Vol. 212, No.1-2, 1993, pp. 43-49.
20. Finckenor M.M., Edwards D.L., Vaughn J.A., Schneider T.A., Hovater M.A., and Hoppe D.T., "Test and Analysis Capabilities of the Space Environment Effects Team at Marshall Space Flight Center", NASA/TP – 2002-212076, 2002.
21. Dooling D., and Finckenor M.M., "Material Selection Guidelines to Limit Atomic Oxygen Effects on Spacecraft Surfaces", NASA/TP – 1999-209260, 1999.
22. Cuthbertson J.W., Langer W.D., and Motley R.W., "Atomic Oxygen Beam Source for Orbital Environments", *Materials & Manufacturing,* Vol. 5, No. 3, 1990, pp. 387-396.
23. Krech R.H., and Caledonia G.E., "AO Experiments at PSI", Report PSI, 1993.
24. Caledonia G.E., Krech R.H., and Green B.D., "A High Flux Source of Energetic Oxygen Atoms for Material Degradation Studies", AIAA Journal, Vol. 25, Jan.1987, pp.59-63.
25. Caledonia G.E.,Krech R.H., Green B.D. and Pirri A.N., US Patent Number 4,894,511, Jan. 16 1990.
26. Cazaubon B., Paillous A., Siffre J., and Thomas R., "Five-Electron-Volt Atomic Oxygen Pulsed-beam Characterization by Quadruple Mass spectrometry", *Journal of Spacecraft and Rockets*, Vol.33, No.6, 1996;
27. Grossman, E., Guzman, I., Viel-Inguimbert, V., and Dinguirard, M., "Modification of 5eV Atomic-Oxygen Laser Detonation Source", *Journal of Spacecraft and Rockets*, Vol. 40, No.1, 2003, pp. 110-113.
28. J. Kleiman, S. Horodetsky, V. Sergeyev, and V. Issoupov, "CO_2-laser assisted atomic oxygen beam sources: Research, development and optimization of operational parameters", Proc. of the 10th Int. Symp. on Materials in a Space Environment and 8th Int. Conf. on Protection of Materials and Structure from the LEO Space Environment, Collioure, France, June 19-23, 2006.
29. Annual Book of ASTM Standards, "Standard practices for ground laboratory atomic oxygen interaction evaluation of materials for space applications", E2089-00.
30. Minton T. et al., "Atomic-Oxygen-Assisted Materials Degradation in LEO: Collisions-Enhanced Erosion, another Synergistic Effect," In Proc. of the 8th Int. Symp. on Material in a Space Environment and 5th Int. Conf. on Protection of Materials and Structure from the LEO Space Environment, Arcachon, France, June 5-9, 2000.
31. Tagawa M., T. Ema, H. Kinoshita, M. Umeno, and N. Ohmae, "Oxidation of Room Temperature Silicon (001) Surfaces in a Hyperthermal Atomic Oxygen Beam", In: Proc. of the 7th Int. Symp. on Materials in a Space Environment. Noordwijk, The Netherlands, 1997, pp. 225-229.
32. Tagawa, M., Yokota, Kumiko, Ohmae, Nobuo, and Kinoshita, Hiroshi, "Volume diffusion of atomic oxygen in α-SiO_2 protective coating", *High Performance Polymers*, Vol. 12, No.1, 2000, pp. 53-63.
33. Tennyson, R. C. "Atomic Oxygen Effects on Polymer-based Materials", Can. J. Phys., 69, 1991, pp. 1190-1208.
34. J. I. Kleiman, Z. Iskanderova, Y. Gudimenko, and S. Horodetsky, "Atomic oxygen beam sources: a critical review." In: Proc. of the 9th Int. Symp. on Materials in a Space Environment. Noordwijk, The Netherlands, 2003, pp. 313-324.
35. Morison, D., Tennyson R.C., and French Y.B. "Microwave Oxygen Atom Beams Source. Fourth European Symposium on Spacecraft Materials in Space Environment", CERT, Toulouse, France, 1988, pp. 435-441.

36. Vaughan J.A., Linton R.C., Carruth Jr. M. R., Whitaker A.F., Cuthbertson J.W., Langer W.D and Motley R.W., "Characterization of a 5-eV neutral atomic oxygen beam facility", in Proceedings of 4th Annual Workshop on Space Operations Applications and Research (SOAR'90), June 26-28, 1990, (1991) pp. 764-771.
37. Auerbach D.J., "Velocity Measurements by Time-of-Flight Methods" in: Atomic and Molecular Beam Methods", V.1. Ed. G. Scoles, Oxford University Press, 1988, pp. 362-379.
38. J. Kleiman, S. Horodetsky, V. Sergeyev, and V. Issoupov, "Space environment simulator. Principles of operation of lateral laser-assisted atomic oxygen source", in preparation.
39. J. Kleiman, S. Horodetsky, V. Sergeyev, and V. Issoupov, "Time-of-Flight measurements of atomic oxygen beam parameters in the laser detonation source", in preparation.
40. Y. Gudimenko, R. Ng, J. Kleiman, Z. Iskanderova, A. Grigorevski, L. Kiseleva, D. Edwards, and M. Finckenor, "Surface modification of conductive and non-conductive thermal control paints: full stabilization for durability enhancement in space environment", Proc. of the 10th Int. Symp. on Materials in a Space Environment and 8th Int. Conf. on Protection of Materials and Structure from the LEO Space Environment, Collioure, France, June 19-23, 2006.